Magnetoreflectance of ferromagnetic metal-insulator granular films with tunneling magnetoresistance

V. G. Kravets
Institute for Information Recording, National Academy of Sciences of Ukraine, 2 Shpak Street, Kiev 03113, Ukraine

L. V. Poperenko
Department of Physics, Taras Shevchenko Kiev National University, 2 Academician Glushkov Avenue, Kiev 03022, Ukraine

A. F. Kravets
Institute of Magnetism, National Academy of Sciences of Ukraine, 36-b Vernadsky Boulevard, Kiev 03142, Ukraine
(Received 16 August 2008; revised manuscript received 7 February 2009; published 9 April 2009)

We present the experimental results on magnetorefractive effect in ferromagnetic metal-insulator granular films of different compositions (identical metals but different dielectric matrices) with tunnel magnetoresistance. It was found that the magnitude of the magnetorefractive effect rises with increasing of the magnetic field but the effect itself strongly depends on the frequency and polarization state of the light. It was revealed that the prominent features on the magnetoreflection spectra in the range of 7.5–10 μm are associated with the excitation of longitudinal phonon modes in the dielectric matrices and accompanying strong electron-phonon interaction which can create the polaron states in the dielectric matrices. The explanation of the magnetorefractive effect in terms of the modified Hagen-Rubens relation has emphasized the importance of the electron-phonon interaction and its relevance both to the tunnel magnetoresistance effect and magnetoreflectance.

DOI: 10.1103/PhysRevB.79.144409 PACS number(s): 75.80.+q, 73.40.Gk, 72.15.Gd

I. INTRODUCTION

Giant magnetoresistance (GMR) effect has been extensively investigated since it was discovered in Fe/Cr multilayer films in 1988 (Refs. 1 and 2) and then in ferromagnetic metal-metal[3] and ferromagnetic metal-insulator (FMI) granular films.[4,5] The magnetoresistance in FMI granular films where electrons tunnel between the metallic magnetic granules through the insulating barriers of the matrix was called tunneling magnetoresistance (TMR). The key property of these materials is the reduction of their electrical resistivity in magnetic field. FMI granular films have attracted attention due to their large TMR.[4–6] This TMR is largely determined by the spin polarization of the tunneling current, which depends not simply on the spin-polarized density of states of the ferromagnetic granules, but also on the spin-dependent relaxation time of the electrons tunneling across dielectric barrier.[7,8] The TMR values of up to ~10% are observed at room temperature in FMI granular films based on 3*d* transition metal (for instance Co-Fe alloys) with tunnel barriers formed by Al_2O_3 and HfO_2.[4,6,9] Al_2O_3 and HfO_2 films as an alternative to SiO_2 have attracted great research attention because of their potential application as a dielectric in microelectronic devices due to their high dielectric constants ($k \approx 8$ and ≈ 25, respectively), wide band gaps, and stabilities.[10] Moreover, these *k*-high dielectrics allow increasing both the gate current and the switching speed of magnetoresistive devices. The influence of the dielectric matrix on the field dependence of the spin-polarized tunneling magnetoresistance of the FMI is of particular interest. Some authors have reported remarkable room-temperature ferromagnetism in nonmagnetic oxides such as HfO_2,[10] TiO_2,[11] and Al_2O_3 (MgO).[12] They supposed that the observed magnetism is due to defect and/or oxygen vacancies. In Ref. 13 it has been proposed that a mechanism could cause magnetic properties in such oxides and the formation of the charge-trapping of polaron states in monoclinic HfO_2 has been shown. The polarons can appear even in a perfect lattice. Such polaron states, which produce a ferromagnetic phase in intrinsic HfO_2, have been predicted theoretically[13] but have never been directly observed. The processes of formation and hopping of polarons between different lattice sites should be very sensitive to external magnetic field and should affect TMR.

One way to check such effect is to study the infrared (IR) reflection/transmission spectra dependence on applied magnetic field. The proposed method is based on the magnetorefractive effect (MRE),[6,14,15] i.e., the variation of the complex refractive index of the FMI films due to a change in its conductivity in the IR region under the influence of the magnetic field. The measurement of the reflection or transmission coefficients of the FMI films allows us to obtain information about their dielectric and electronic properties. Hence, IR reflection spectroscopy in magnetic field is a direct tool to probe the spin-dependent conductivity in FMI granular films. Usually, the measurements are performed in reflection mode because it is the most suitable variant for practical remote sensing of TMR.[14,15] It is necessary to note that the wavelength profile of the MRE spectra demonstrates the strong sensitivity to GMR material parameters.[9,15]

One of the interesting problems in the area of the electron transport in the metal-insulator granular films is the influence of electron-phonon (*e-p*) scattering on the tunneling current. Additional satellite peaks have been observed on the current-voltage (*I-V*) curves.[16] These peaks are generally attributed to the emission of optical phonons in insulating matrix by tunneling electrons.[6,16] These investigations have shown that the optical phonon modes on the interface between ferro-

magnetic particles and insulator matrix play an important role in the magnetotransport of such systems.

We have previously shown that the optical and magneto-optical properties of the FMI CoFe-AlO(HfO) granular films in spectral region 0.2–1 μm (uv-visible-near IR) are not sensitive to their magnetoresistance effect.[6,17] In study[6] only the MRE effect for p-polarized light in CoFe-Al_2O_3 granular films as a function of wavelengths and compositions of films was investigated. The main attention was paid on the excitation of longitudinal optical (LO) phonon modes and found that these modes could be significantly enhanced in external magnetic field. However, in this work the nature of MRE in CoFe-Al_2O_3 granular films was not fully discussed. The major achievement presented in present paper is a complete analysis of the MRE for broad class of the FMI granular films, providing physical origin of this effect. We extend previous experimental measurements[6] on the $(CoFe)_x(HfO_2)_{(1-x)}$ magnetic granular films with TMR-like properties and high dielectric constant. In present work the idea of using polaron model for describing the MRE in the FMI granular films and multilayer FM/I/FM structures with TMR effect has been discussed.

Here we present an evidence of the electron-phonon coupling in the FMI CoFe-AlO(HfO) granular films which is obtained from analysis of the magnetic field dependence of intensity of the IR active LO phonon modes. It was shown that the dependence of MRE on a polarization state of light gives the possibility to separate the contributions from ferromagnetic granules and nonmagnetic insulator to both magnetic and magnetoresistance properties of such materials. The measurement of the MRE of the FMI granular films allows us to obtain information about the interaction of tunneling electron with LO phonons as well as a formation of electronic quasiparticles such as polarons. To understand correctly the field dependence of the scattering coefficient of the FMI granular films the contributions from longitudinal optical phonons should be taken into consideration. The variation of the reflectivity in the LO phonon excitation area with the magnetic field changing can be precisely reproduced in this case. The MRE in the IR, which is closely related to the TMR, was used to study of magnetotransport properties of the FMI films. The way of direct control magnetic state of nonmagnetic oxides by measuring of the magnetoreflectance at uniquely determined resonant wavelengths in the middle IR region has been proposed in this article. This study is of primary importance for applications of such materials in photospintronics devices and magnetophotonic crystals.

II. EXPERIMENTAL PROCEDURE

The $(Co_{0.5}Fe_{0.5})_x(Al_2O_3)_{1-x}$ and $(Co_{0.5}Fe_{0.5})_x(HfO_2)_{1-x}$ granular films (where $x=0.07-0.49$ is the volume fraction of $Co_{0.5}Fe_{0.5}$) of thickness ~200 nm were codeposited using e-beam evaporation from $Co_{0.5}Fe_{0.5}$ and Al_2O_3 (HfO_2) independent sources onto glass substrates. The pressure was less than 10^{-4} Pa during the film deposition. The composition of the films was determined using energy dispersive x-ray analysis. The crystalline structure was investigated by x-ray diffraction (XRD) and transmission electron microscopy (TEM). The room-temperature (RT) magnetoresistance was measured using standard four-point probe technique with both current and applied magnetic field H in the film planes. In- and out-plane magnetic hysteresis loops were measured at RT using an Oxford vibrating sample magnetometer.

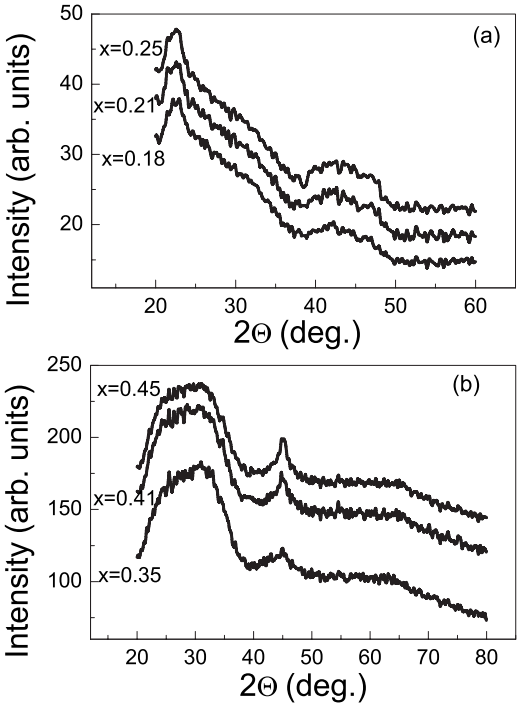

FIG. 1. XRD patterns of as-prepared (a) $(CoFe)_x(Al_2O_3)_{1-x}$ and (b) $(CoFe)_x(HfO_2)_{1-x}$ granular films.

IR reflection spectra were recorded within 2.5–25 μm region using a Fourier transform IR reflection spectrometer with 4 cm^{-1} resolution and liquid-nitrogen-cooled HgCdTe detector. The angle of light incidence with respect to the film normal was equal to 65°. MRE measurements were performed in magnetic field up to 12 kOe. The incident light was polarized using a KRS-5 grid polarizer. In order to detect a fine magnetic field-dependent features, reflectance ratios $\Delta R/R=[R(H)-R(H=0)]/R(H=0)$ have been calculated. The magnetic field vector H was perpendicular to the propagation direction of the IR radiation and parallel to the film surface. Data were averaged over 400 separate runs. It has been checked that the reflectance of Ag and Al reference mirrors does not depend on magnetic field.

III. EXPERIMENTAL RESULTS

Figures 1(a) and 1(b) show the XRD spectra of CoFe-Al_2O_3 and CoFe-HfO_2 granular films, respectively. Two broad maxima with a half width of about 3°–5° around 33° and 44° can be observed in the as-prepared CoFe-HfO_2 films suggesting that the films contain two disordered phases, which have a nanocrystalline and/or amorphous structure. A low-angle peak can be assigned to the dielectric matrix structures whereas the peak at the Bragg angle ~44° corresponds to the metallic nanostructure.[18] This broad peak indicates also nanocrystallinity of the metal clusters in Al_2O_3 or HfO_2

matrix [Figs. 1(a) and 1(b)]. The intensities of these lines increase and the crystalline structure becomes more ordered while the concentration of CoFe increases. Meanwhile, the intensities of HfO_2 (33°) and Al_2O_3 (25°) lines decrease [Figs. 1(a) and 1(b)]. It witnesses the formation of the large number of CoFe alloy clusters in granular films.

Assuming a nanocrystalline structure, the angle positions of the peaks in Figs. 1(a) and 1(b) may correspond to CoFe (110) and HfO_2 (111) or Al_2O_3 (111) lattice spacings, as suggested in Ref. 18. Therefore, two phases can be attributed to the HfO (AlO)-rich and the CoFe-rich phases. The coherence length and thus the size of the nanocrystals were estimated from the half width of peaks using the Scherer's formula[19] as ≈3–5 nm. Thus, the nanocrystal size is comparable to the radius of the short-range order for amorphous materials.[20] The two broad peaks shift away from each other with the increasing metallic component in the granular films while their half widths decrease slightly. These results demonstrate that a phase separation and a structural relaxation take place. Note that the amorphousness is a desirable property for *k*-high gate oxide materials. The amorphous phase of a representative *k*-high materials, HfO_2 (Al_2O_3), has been found to have a higher dielectric constant than the monoclinic crystalline phase.[21] The enhancement in the dielectric constant (ε) is largely due to the increase in lattice polarization with a softening of the phonon modes rather than to an increase in electronic polarization. Such transformation of phonon modes will be studied in this work using the IR spectroscopy technique.

The resistivity measurements show that the electrical percolation (the transition from metallic-type electron transport to insulator-type one) occurs at $x_p \sim 0.35$ for the $(CoFe)_x(HfO_2)_{1-x}$ system and at $x_p \sim 0.18$ in the $(CoFe)_x(Al_2O_3)_{1-x}$ granular films. There is no dependence of TMR in the different geometries so the systems are isotropic. The maximum values of TMR of about 7.5% and 4.3% in the magnetic field 8.2 kOe and at RT are observed for $(CoFe)_x(Al_2O_3)_{1-x}$ and $(CoFe)_x(HfO_2)_{1-x}$ granular films, respectively. Maximal TMR effects are observed for $x_p \sim 0.18$ in $(CoFe)_x(Al_2O_3)_{1-x}$ and for $x_p \sim 0.35$ in $(CoFe)_x(HfO_2)_{1-x}$. According to previous works,[4–8] the main contribution to TMR is due to tunneling of the spin-polarized electrons in metal-dielectric films. It should be noted that these compositions are closed to the estimated value of percolation threshold.

The magnetization (M) versus magnetic field (H) measured at RT for $(CoFe)_x(Al_2O_3)_{1-x}$ and $(CoFe)_x(HfO_2)_{1-x}$ granular films is shown in Fig. 2. One can see from this figure that the $(CoFe)_x(Al_2O_3)_{1-x}$ samples with the volume fraction $x=0.18$, 0.21, and 0.25 of CoFe are ferromagnetic. The coercive field $H_c \sim 70$ Oe is observed for films with $x=0.21$. The saturation magnetization M_s is of 350 emu/cm^3. This value is a little bit low taking into account relatively high content of Al_2O_3 in the films. A value between 500 emu/cm^3 and 700 emu/cm^3 was measured for a lower Al_2O_3 content ($x=0.35-0.5$). The measured coercive field, $H_c=63$ Oe, is relatively high for amorphous or nanocrystalline structure. At low concentration of CoFe ($x<x_p$) $M(H)$ curves exhibit a typical superparamagnetic behavior (the plots are not shown here). The hysteresis loop of the

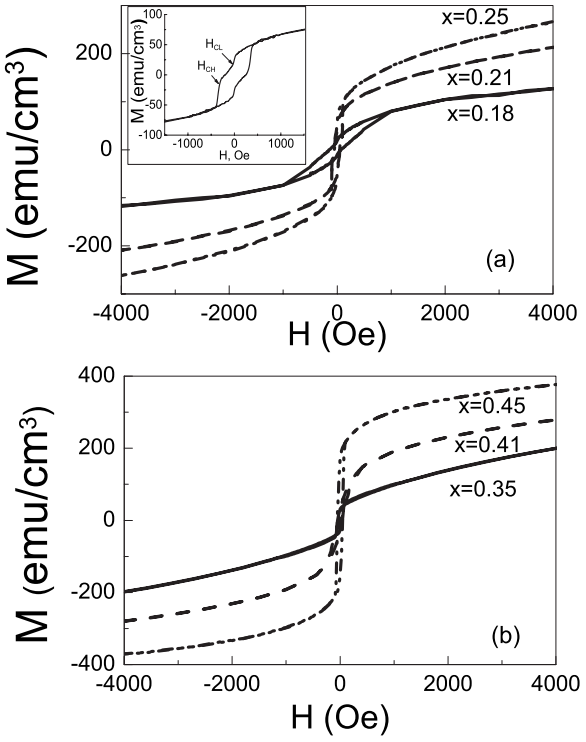

FIG. 2. Hysteresis loops measured at RT for (a) $(CoFe)_x(Al_2O_3)_{1-x}$ and (b) $(CoFe)_x(HfO_2)_{1-x}$ granular films with different metallic concentration. Inset shows the hysteresis loop of the $(CoFe)_x(Al_2O_3)_{1-x}$ films with $x \approx x_p$.

$(CoFe)_x(Al_2O_3)_{1-x}$ films with $x \approx x_p$ is presented in the inset of Fig. 2(a). This loop is characteristic for two magnetic phase materials. One phase seems to be a CoFe-rich phase with a small saturation M_s and another phase with nearly linear $M(H)$ dependence and $H_s > 700$ Oe seems to be a uniaxial anisotropic system with H along the hard axis. As a result, the shape of hysteresis loop is modified monotonous to steplike one. It is possible to distinguish in Fig. 2 two "coercive" fields: H_{c1} for small magnetic fields and H_{c2} for larger ones [see inset Fig. 2(a)].

Figure 2(b) shows three magnetization loops measured for the $(CoFe)_x(HfO_2)_{1-x}$ granular films with $x=0.35$, 0.41, and 0.45, respectively. The room-temperature ferromagnetic ordering takes place in these films. These granular films demonstrate almost isotropic magnetic properties with decreasing coercivity, H_c, for CoFe-rich amorphous alloys. Experimental data [Fig. 2(b)] show the presence of significant coercivity and remanence. The coercive fields are in 30–50 Oe range and decrease with x decreasing. It was found that the easy direction of the magnetization in $(CoFe)_x(HfO_2)_{1-x}$ granular films is in the film plane. The saturation magnetization determined from the $M(H)$ curve is of 450 emu/cm^3. Magnetization measurements indicate that, with decreasing x, $(CoFe)_x(HfO_2)_{1-x}$ films transform from ferromagnet to superparamagnet around $x<0.35$.

Such results obtained suggest that the films consist of two disorder phases, namely, a CoFe-rich and a AlO (HfO)-rich one. For concentration ferromagnetic particles below percolation threshold, x_p, samples showed superparamagnetic behavior as can be expected for noninteracting small particles.

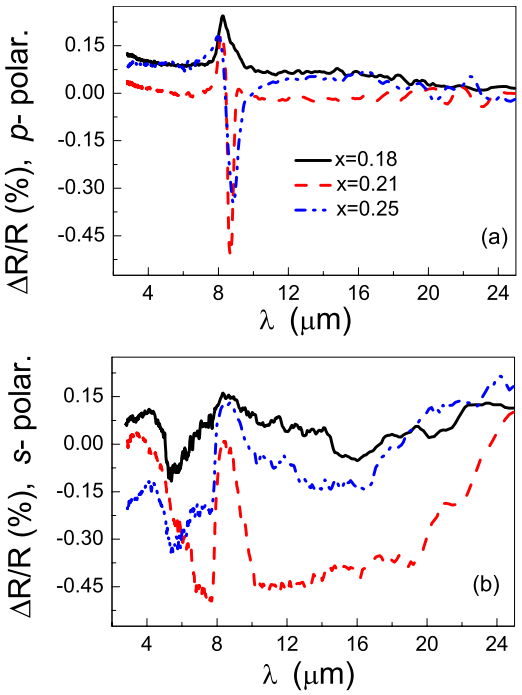

FIG. 3. (Color online) The MRE spectra for the $(CoFe)_x(Al_2O_3)_{1-x}$ granular films with different metallic concentration for $H=12$ kOe: (a) p-polarized light; (b)s-polarized light.

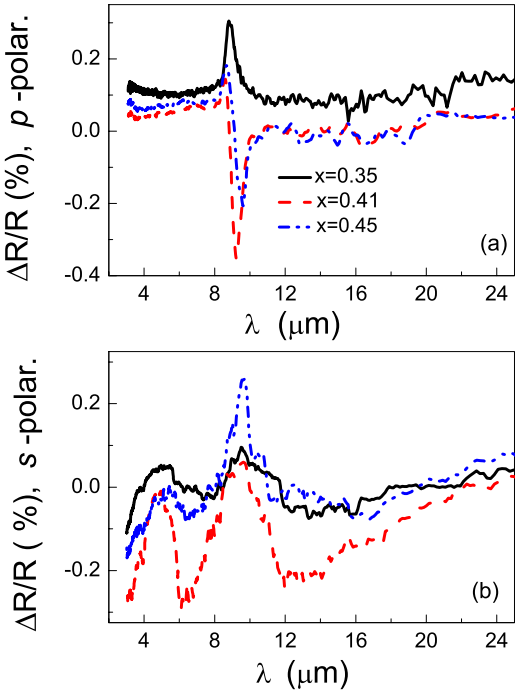

FIG. 4. (Color online) The MRE spectra for the $(CoFe)_x(HfO_2)_{1-x}$ granular films with different metallic concentration for $H=12$ kOe: (a) p-polarized light; (b) s-polarized light.

For $x>x_p$ the films consist of two magnetic phases: a phase with a large coercivity and relatively low remanence which is typical for large ferromagnetic particles and another with a low coercivity and high remanence.

The correlation between reflectivity and electrical resistance was studied to investigate the possibility to measure magnetoresistance using MRE. Figure 3 shows the relative change of the IR reflection, $\Delta R/R$, for $(CoFe)_x(Al_2O_3)_{1-x}$ films with different x in the magnetic field $H=12$ kOe as a function of a wavelength for p- and s-polarized incident lights, respectively. For low concentration of CoFe the MRE is essentially larger for p-polarized light than for s-polarized one. Polarization measurements of the MRE show that for films enriched by Al_2O_3 ($x\leq x_p$) the MRE is mostly determined by the p polarization while for $x>x_p$ both s and p polarizations contribute to the MRE value. In the case of $x\leq x_p$, p-polarized incident light MRE spectra (Fig. 3) have similar shape with single local maximum at $\lambda\sim 8.0-8.5$ μm, while for $x>x_p$ there is a pronounced dip in the reflection in the spectral region of 8.5–9.2 μm. The position of the dip is shifted toward longer wavelength λ whereas the volume CoFe content increases (see Fig. 3). The significant change in intensity of the dip at $\lambda\sim 8.0-8.5$ μm and a weak increase in linewidth were observed with increasing magnetic field. In contrast, the spectral dip position ($\lambda\sim 8.5$ μm) does not change. Thus, in the granular films MRE changes sign when their composition passes through the percolation threshold. So, it is possible to determine the percolation point from the MRE measurements.

Figure 4 presents the relative change of the IR reflection for $(CoFe)_x(HfO_2)_{1-x}$ granular films in the magnetic field $H=12.0$ kOe as a function of wavelength for both polarizations of incident light. As one can see [Fig. 4(a)], the MRE spectra of $(CoFe)_x(HfO_2)_{1-x}$ granular films for p-polarized incident light has a single local minimum at $\lambda\sim 9.0-10.0$ μm while for s-polarized light [Fig. 4(b)] the magnetoreflection has a pronounced maximum within the same spectral range. It was found that the amplitude of the MRE peaks increases while the magnetic field intensity rises.

Our experiments have shown that for p-polarized incident light the MRE spectra of $(CoFe)_x(Al_2O_3)_{1-x}$ and $(CoFe)_x(HfO_2)_{1-x}$ granular films have a similar shape with a single local minimum at $\lambda\sim 8.2-8.7$ μm and $\lambda\sim 9.3-10.0$ μm, respectively. Hence, the position of the extrema of the MRE spectra is shifted toward larger wavelength, λ, with the increase of CoFe volume content in granular films. At the same time, in the MRE spectra for s-polarized light, there is a sharp magnetoreflectivity minimum at $\lambda\sim 6.0-8.0$ μm and a broad maximum at $\lambda\sim 9.0$ μm for $(CoFe)_x(Al_2O_3)_{1-x}$ granular films. For $(CoFe)_x(HfO_2)_{1-x}$ films the s-polarized MRE dependence exhibits double peak resonance behavior within 4–11 μm range. The positions of the dips are slightly changed with x increasing while the position of the maxima are very stable.

The analysis of the measured MRE spectrum shows that their absolute magnitudes and shapes strongly depend on a polarization of incident light. For p-polarized light the MRE displays the extremal values of about $\sim 1.2-1.5$ times larger than for s-polarized light ones. The characteristic feature of p-polarized MRE in FMI granular films is very narrow resonance. It is important to be noted that the magnetoreflectance spectra of s-polarized light in the low-wavelength region are similar to that observed in CoAg granular films.[14] It is due to

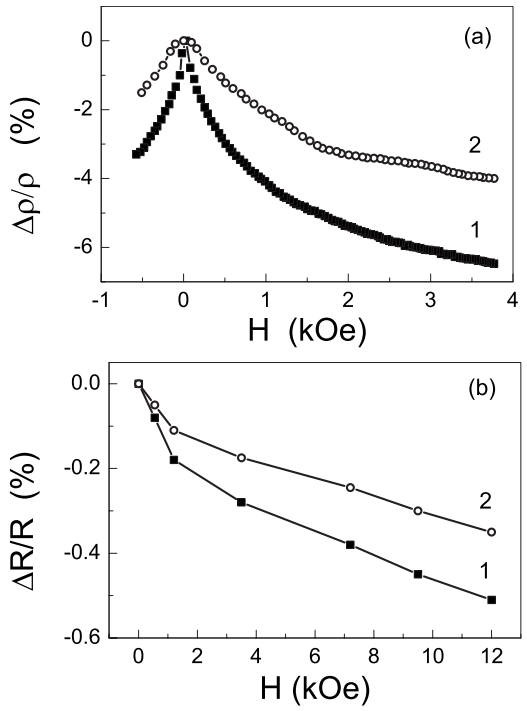

FIG. 5. (a) Experimental $\Delta\rho/\rho$ data for (1) $(CoFe)_{0.21}(Al_2O_3)_{0.79}$ and (2) $(CoFe)_{0.41}(HfO_2)_{0.59}$ granular films; (b) measured p-polarized MRE vs magnetic field at fixed wavelength ($\lambda=8.6$ μm) for (1) $(CoFe)_{0.21}(Al_2O_3)_{0.79}$ and ($\lambda=9.3$ μm) for (2) $(CoFe)_{0.41}(HfO_2)_{0.59}$ granular films.

the Drude contribution from the intraband transitions of free electrons in the magnetic granules. The observed sharp dip and/or maximum in the measured MRE spectra of these CoFe-based systems may be attributed to a response of the longitudinal optical LO vibration mode of atomic pairs Al-O (Hf-O) or of atomic groups "transition metal"–"aluminum (hafnium)"–"oxygen" [TM-Al (Hf)-O].[6,12,16] For example, when the oxygen vacancy is at the HfO_2/CoFe interface, it is easily substituted by the Fe or Co atom to form an Co(Fe)-Hf-O bonding. This could also slightly change the IR phonon modes. It should be noted that pronounced dips appear on the reflectivity spectra of the studied FMI films when a LO phonon is excited. The dip becomes more pronounced and its magnitude increases nonlinearly when the magnetic field increases. The relative decrease of $R(\lambda)$ in this spectral range under external magnetic field correlates with magnetoresistance behavior.

Figure 5 shows the high correlation between the electrically measured TMR and the optically measured MRE for FMI granular films. The difference in dielectric matrix (Al_2O_3 or HfO_2) leads to different values of the TMR effect [Fig. 5(a)]. The measurements of the MRE profiles were carried out at fixed wavelength when the magnetoreflectance reaches a maximum. The experiment was performed by direct recording of the changes in the reflected p-polarized beam as a function of applied magnetic field H at $\lambda\sim8.6$ μm and $\lambda\sim9.3$ μm for $(CoFe)_x(Al_2O_3)_{1-x}$ and $(CoFe)_x(HfO_2)_{1-x}$ granular films, respectively [Fig. 5(b)]. It has been previously shown[14,22] that the correlation between the GMR and MRE should be most evident at extreme wavelengths where the MRE reproduces the maximum values. These dependences [Figs. 5(a) and 5(b)] clearly show the possibility to perform noncontact magnetotransport measurements on the samples with tunneling magnetoresistance by measuring the variation of their infrared reflected intensity in magnetic field at fixed λ. Moreover, our measurements show that the tunneling magnetoresistance as well as a magnetoreflectance is approximately proportional to the square of the magnetization, which allows us to extract a measure of $M(H)$ from optical data in the IR. Thus, the existence of ferromagnetism in the nonmagnetic oxides as well as the nature of the spin-lattice interaction or formation of polarons could be confirmed.

IV. MODEL AND DISCUSSION

The obtained results demonstrate that the observed magnetoreflective phenomena are due to a collective reflection of light in the nanogranular film ensemble. To describe the interaction between the incident light and the granular films we use the effective-medium approximation (EMA) by assigning a complex effective index of the refraction to our structure.[23,24] The effective complex dielectric function, ε_{eff}, for a composite system containing metal particles embedded in a host matrix is defined by relationship

$$\varepsilon_{\text{eff}}=\varepsilon_d\frac{\varepsilon_m(1+2x)+2\varepsilon_d(1-x)}{\varepsilon_m(1-x)+\varepsilon_d(2+x)}, \tag{1}$$

where ε_{eff}, ε_d, and ε_m are the effective complex dielectric functions of granular film, dielectric (Al_2O_3 or HfO_2), and metallic (CoFe) media, respectively; x is a metal volumetric concentration. The dielectric function of CoFe alloy, ε_m, can be divided into a free-electron part ε_m^f and an interband part ε_m^i; i.e., $\varepsilon_m=\varepsilon_m^f+\varepsilon_m^i$. The intraband electrons mostly affect on the effective refractive indexes in the middle IR spectral region. As a result, the Drude's model can be used to find ε_m^f (Ref. 25)

$$\varepsilon_m^f=\varepsilon_r-\frac{i\omega_p^2\tau}{\omega(1-i\omega\tau)}. \tag{2}$$

Here, ω_p is the "quasifree" plasma frequency of CoFe, τ is the conduction-electron relaxation time, and ε_r is the relative dielectric constant of the alloy, which is contributed by bound electrons. The plasma frequency, ω_p, and relaxation time, τ, of conduction electron for pure CoFe film were extracted from ellipsometric measurements in the far IR as well as a value of dc resistivity, ρ_0.

In the midinfrared region, where optical phonons can be excited, the dielectric function ε_d of insulating Al_2O_3 or HfO_2 can be approximated by a phenomenological Lorentz oscillator model[12,26,27]

$$\varepsilon_d=\varepsilon_\infty\prod_j\frac{\nu_{\text{LO}j}^2-\nu^2-i\nu\gamma_{\text{LO}j}}{\nu_{\text{TO}j}^2-\nu^2-i\nu\gamma_{\text{TO}j}}, \tag{3}$$

where ε_∞ is the high-frequency dielectric function. The vibrating frequencies and Lorentz widths of the LO and TO modes are $\nu_{\text{LO}j}$, $\nu_{\text{TO}j}$ and $\gamma_{\text{LO}j}$, $\gamma_{\text{TO}j}$, respectively. For our

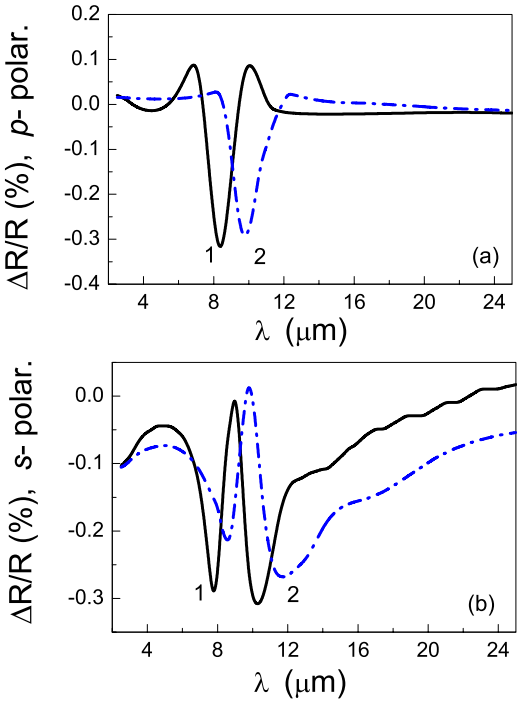

FIG. 6. (Color online) The calculated values of the MRE vs the wavelength for (a) *p*- and (b) *s*-polarized lights: (1) $(CoFe)_{0.21}(Al_2O_3)_{0.79}$ and (2) $(CoFe)_{0.41}(HfO_2)_{0.59}$ granular films.

calculation only two pairs of phonon modes (LO/TO, $j=1,2$) were considered.

Using Eqs. (1)–(3) for ε_m^f and ε_d, we determined the effective dielectric function ε_{eff} and the effective complex refraction index $n_{\text{eff}}+ik_{\text{eff}}$ which can be used to calculate the optical response of the samples. The effective dielectric function ε_{eff} contains a plasma term due to the free carriers of individual metallic grains and additional resonant term with longitudinal optical and transverse optical modes. Then the reflectance spectra were calculated using the Fresnel equations for the three-layer system: air, uniform layer of granular films (effective medium), and thick glass substrate. The only parameters in the calculations are the thickness of the granular films and the dielectric constants of metal and insulating films.

Experimental results show that the MRE in FMI granular films occurs only for films with significant TMR effect. According to the Hagen-Rubens relation,[25] the TMR and MRE are connected to each other and the reflectivity is a function of the dc resistivity, ρ_0, $R=1-[2\varepsilon_0\omega\rho_0]^{1/2}$, where ε_0 is the permittivity of a free space. The change in the reflectivity $\Delta R/R$ can be obtained as a first derivation of R

$$\frac{\Delta R}{R} = -\frac{[2\varepsilon_0\omega\rho_0]^{1/2}}{1-[2\varepsilon_0\omega\rho_0]^{1/2}} \times \frac{\Delta\rho}{2\rho_0} = -\frac{1-R}{R} \times \frac{\Delta\rho}{2\rho_0}, \quad (4)$$

where $\Delta\rho/\rho$ is the TMR for the granular films. It is evident from Eq. (4) that $\Delta R/R$ depends on tunnel magnetoresistance, $\Delta\rho/\rho$.

Figure 6 displays the theoretical magnetoreflectance of the granular films as a function of the wavelength for maximal values of tunnel magnetoresistance $\Delta\rho/\rho$ [Fig. 5(a)]. The shape and spectral positions of the dips for the MRE spectra of *p*-polarized light [Figs. 3(a) and 4(a)] are well described by our theoretical model [Fig. 6(a)]. For *p*-polarized light there are three regions. In two regions of 2.5–6.5 and 12–25 μm the magnitude of MRE is close to zero, and in region of 6.5–11 μm, the magnitude of $\Delta R/R$ reaches the minima. At the same time, in the MRE spectra for *s*-polarized light there is a sharp magnetoreflectivity maximum in aforementioned spectral region [Fig. 6(b)]. It is worth to be noted that the spectral behaviors of effective complex refraction index $n_{\text{eff}}+ik_{\text{eff}}$ correlate with dependence of $\Delta R/R$. The abrupt change of $\Delta R/R$ in the areas $\lambda\sim 8.5-9.0$ μm and $\lambda\sim 9.3-10.0$ can be explained by a drop of k_{eff} to small values. Hence, effective-medium approach leads to a dielectriclike behavior of FMI granular films in the region of LO phonons excitation. Our attention was focused on the dips at $\lambda\sim 8.5-9.0$ μm and $\lambda\sim 9.3-10.0$ μm [Fig. 6(a)] which can be associated with the LO optical modes because they are close to the appropriate frequencies.[26,27] Practically, the complex dielectric function for this system can be expressed in term of the Drude-type wavelength dependence, which yields electron-phonon scattering and plasma frequencies. The decrease of the reflectivity in the vicinity of the LO phonon energy while magnetic field intensity enhances is extremely well reproduced by our analysis.

Experimental results are very interesting since large changes in the compositions (HfO_2 in comparison to Al_2O_3) produce small change in magnetic field tendency of MRE. From structural point of view, amorphous Al_2O_3 has a corundum structure with trigonal (or rhombohedral) unit cell containing two Al_2O_3 molecules. The coordinates of the atoms are such that an Al atom is surrounded by six O atoms of two different nearest-neighbor (NN) distances and each O atom has four NN Al atoms.[28] The electron densities between Al and O at normal sites exhibit a typical ionic character of bonding. However, the electron densities of O_i^{2-} undergo significant distortion due to interactions with their neighboring ions. Such electronic interactions will affect its defect-formation energy. In contrast to Al_2O_3, pure HfO_2 is monoclinic at room temperature. There are two kinds of oxygen atoms, which have different coordinations: O (1) having three NN Hf between 2.04 and 2.15 Å and O (2) having four NN Hf between 2.16 and 2.26 Å. The theoretical calculation and experiment studies show that the hafnium oxide is an ionic insulator with some degree of covalent bonding between Hf and O atoms.[29] Recent reports on ferromagnetism in undoped HfO_2 films have led to the development of model which is based on the formation of bound magnetic polarons associated with oxygen vacancies in a dielectric matrix.[30] These results suggest that the intrinsic ferromagnetism in HfO_2 is thought to arise from lattice defects. Further, the energy position of the defect level is found to depend on the atomic arrangements after the vacancy formation. The reduction in the mean Hf-O bond length (~0.1 Å, as predicted in Ref. 13) and in the number of bonds in the presence of oxygen vacancy will influence the detailed balance in the charge dynamics between two atomic species. It was shown that the Al-O bonds could be shorter by about 0.2 Å due to the formation of oxygen vacancies in a dielectric matrix.[28] In pres-

ence of vacancies for Hf (Al) and O, extra levels were induced around conduction-band edges in the band gap of wide semiconductors. It was found that the oxide vacancies moved out from symmetry site and these displacements are small (0.1–0.2 Å) but due to them it is possible to perform of polaron states.

In Ref. 13 stable polaron states in perfect monocline HfO_2 were predicted due to small elongation of the Hf-O bonds, similar to the appearance of oxygen vacancy. These displacements and vacancies in HfO_2 could form high-spin defect states and therefore they could be coupled ferromagnetically and create a ferromagnetic ground polaron states. It is interesting to note that self-trapping energies for polaron states of HfO_2 lie in the range between 0.03 and 0.25 eV according to Ref. 13. This is similar to the polaron binding energy $E_p \approx 0.13$ eV ($E_p = \alpha \hbar \nu_{LO}$, where α is the electron-phonon coupling constant and ν_{LO} is the frequency of LO phonon mode of HfO_2) obtained in our experiments for the $(CoFe)_x(HfO_2)_{1-x}$ granular films. Based on framework of the polaron theory within the intermediate coupling regime ($1 \leq \alpha \leq 5$) the binding polaron energy $E_p \sim 0.17$ eV for $(CoFe)_x(Al_2O_3)_{1-x}$ granular films has been estimated. Thus, our experimental measurements show that the polaron levels locate at distance of about 0.1–0.2 eV from top of band gaps for amorphous HfO_2 and Al_2O_3.

In order to explain coherent emission of phonons under magnetic field for FMI structures, we have also considered the polaron dynamic in external magnetic field. The word "coherent emission" was used in a sense of sharp frequency response of the reflectivity on the applied magnetic field. We have observed the resonances in $\Delta R/R$ spectra which occur at discrete frequencies and are strongly dependent on type of dielectric matrix and metallic volume fraction. Electrons in sapphire-type oxides can form polaron states due to a strong interaction between the conduction electrons and LO phonons.[12,13] Such oxide is a material with the documented strong interaction between the electrons and longitudinal optical phonons. This interaction leads to self-created potential wells, which localize the electrons in the band gap, thereby forming polarons.[12] In this context, we assume that the observed wavelength dependence of the magnetoreflectivity is a manifestation of the dependence of polaron scattering rate on the magnetic field applied. Under the action of the magnetic field the electrons in the system can gain the energy from magnetic field applied and from the phonon absorption scattering process and lose the energy through emitting phonons. From the fitting of the polaron theory to the experimental reflection and magnetoreflection data, it was found that the polaron binding-energy shifts slightly in comparison to LO phonon energy, $\hbar \nu_{LO}$. Moreover, the magnetoreflectance in the mid-IR region displays a reaction of two separated phases on external magnetic field, namely, CoFe contribution and AlO (HfO) contribution in MRE. The metallic behavior dominates in the magnetoreflectance for high-energy region (see Figs. 3–6). In near and middle IR (3–6 μm) the absolute magnitude of the *s*-polarized MRE for all the samples decreases with increasing wavelength due to scattering of conduction electrons on the metallic granule interfaces. It follows from comparison of MRE dependence of FMI granular films and CoAg granular films.[14,22] The experimental data on MRE clearly indicate the existence of spin-dependent tunneling at high energies (at least up to near IR region). This became evident from the correlation of field and concentration dependences of the TMR and MRE for these granular films. However, there are some peculiarities that cannot be explained by model, which establish a connection between the MRE and TMR as a function of CoFe content in the films. The resonance features in the MRE spectra for both polarizations appear due to polaronlike trapping near oxygen vacancies in insulator HfO_2 or Al_2O_3.[10–13,30] The measured MRE spectra of the granular films show the complex character of the optical vibration modes of Hf-O and Al-O molecules. It indirectly indicates the existence of an additional mechanism of MRE in metal-insulator granular films, which is probably connected with magnetic excitations (polaron states) in the AlO or HfO matrix. The existence of two-phase behaviors in magnetic hysteresis loops (Fig. 2) confirms this conclusion. It seems that strong magnetic correlations among particles take place through matrix and the out-of-plane stripelike domain structure is responsible for the strong demagnetizing interactions in metal-insulator granular films. Moreover, the polaron states in the Al_2O_3 and HfO_2 barriers of FMI granular films can introduce two-step tunneling: the normal spin-coherent tunneling process and noncoherent one. Here "coherent" and "noncoherent" are referring to the Bloch symmetry.[31] In the coherent tunneling process both the electrons' spins and their Bloch states symmetry are conserved. Oxygen vacancies in dielectric films are known to contribute to the increase of the overall resistance. Such additional scattering of tunneling electrons inside the dielectric barrier can lead to lower tunnel magnetoresistance. In particular, oxygen point defects located in matrix HfO_2 or Al_2O_3 are predicted to decrease the difference between the spin-up and spin-down transmission coefficients[32] in the barrier, thereby the tunneling magnetoresistance will be reduced.

V. CONCLUSIONS

The possibility to observe the changes in intensity of the IR active longitudinal optical phonon modes for CoFe-HfO_2 and CoFe-Al_2O_3 granular films in magnetic field has been experimentally demonstrated here. It was found that the enhancement of the emissivity at longitudinal phonon modes in external magnetic field could be a common characteristic for all class of FMI-like granular films. The position of dips of the reflectivity spectra in the middle IR region strongly depends on the light polarization and type of matrix (HfO_2 or Al_2O_3). There is a high degree of correlation between the TMR and MRE in FMI granular films. There are two contributions to the magnetoreflectance in the middle IR region in external magnetic field from two separated phases: CoFe contribution and AlO (HfO) one. It has been shown that $\Delta R/R$ spectra for metal-insulator films consist of two components: a discrete structure, which appears due to electron-phonon coupling at $\lambda \sim 8.5–10$ μm, and metalliclike background over all spectral regions. The wavelength dependence of the magnetoreflectivity is a manifestation of direct dependence of electron-tunneling scattering rate and the LO pho-

non excitations on the magnetic field amplitude. The separation of two magnetic phases in the metal-insulator granular films confirms the strong dependence of the MRE spectra on polarization state of incident light.

We have concluded that the MRE spectra in the middle IR region are a very sensitive to the details of magnetic properties of the ferromagnetic metal-insulator films and they can be used experimentally for noncontact measurements of TMR with high surface resolution (in case of focusing light to a size of λ). It was shown that a phenomenon of resonant enhancement of the LO phonon modes in the IR spectra of nonmagnetic oxides can be used to detect and to study their ferromagnetic properties. It may be the important step to a direction of the best understanding of the nature of such kind of ferromagnetism.

ACKNOWLEDGMENTS

The authors would like to thank V. Golub for his helpful discussion. This work was supported by the Ukrainian Program "Nanostructural Systems, Nanomaterials, Nanotechnology" under Project No. 7-08/H.

[1] M. N. Baibich, J. M. Broto, A. Fert, F. Nguyen Van Dau, F. Petroff, P. Etienne, G. Creuzet, A. Friederich, and J. Chazelas, Phys. Rev. Lett. **61**, 2472 (1988).
[2] G. Binasch, P. Grünberg, F. Saurenbach, and W. Zinn, Phys. Rev. B **39**, 4828 (1989).
[3] A. E. Berkowitz, J. R. Mitchell, M. J. Carey, A. P. Young, S. Zhang, F. E. Spada, F. T. Parker, A. Hutten, and G. Thomas, Phys. Rev. Lett. **68**, 3745 (1992); J. Q. Xiao, J. S. Jiang, and C. L. Chien, Phys. Rev. Lett. **68**, 3749 (1992).
[4] J. Inoue and S. Maekawa, Phys. Rev. B **53**, R11927 (1996).
[5] H. Fujimori, S. Mitani, and S. Ohnuma, Mater. Sci. Eng., B **31**, 219 (1995); A. Milner, A. Gerber, B. Groisman, M. Karpovsky, and A. Gladkikh, Phys. Rev. Lett. **76**, 475 (1996); S. Mitani, S. Takahashi, K. Takanashi, K. Yakushiji, S. Maekawa, and H. Fujimori, *ibid.* **81**, 2799 (1998).
[6] V. G. Kravets, L. V. Poperenko, I. V. Yurgelevych, A. M. Pogorily, and A. F. Kravets, J. Appl. Phys. **98**, 043705 (2005); V. G. Kravets, A. N. Pogorely, A. F. Kravets, A. Ya. Vovk, and Yu. I. Dzhezherya, Phys. Solid State **45**, 1530 (2003).
[7] M. Julliere, Phys. Lett. **54A**, 225 (1975).
[8] J. G. Simmons, J. Appl. Phys. **34**, 1793 (1963).
[9] A. B. Granovsky, I. V. Bykov, E. A. Gan'shina, V. S. Gushchin, M. Inoue, Yu. E. Kalinin, A. A. Kozlov, and A. N. Yurasov, JETP **96**, 1104 (2003).
[10] M. Venkatesan, C. B. Fitzgerald, and J. M. D. Coey, Nature (London) **430**, 630 (2004).
[11] S. D. Yoon, Y. Chen, A. Yang, T. L. Goodrich, X. Zuo, D. A. Arena, K. Ziemer, C. Vittoria, and V. G. Harris, J. Phys.: Condens. Matter **18**, L355 (2006).
[12] V. G. Kravets, Phys. Rev. B **72**, 064303 (2005).
[13] D. Munoz Ramo, A. L. Shluger, J. L. Gavartin, and G. Bersuker, Phys. Rev. Lett. **99**, 155504 (2007).
[14] V. G. Kravets, D. Bozec, J. A. D. Matthew, S. M. Thompson, H. Menard, A. B. Horn, and A. F. Kravets, Phys. Rev. B **65**, 054415 (2002).
[15] J. C. Jacquet and T. Valet, in *Magnetic Ultrathin Films, Multilayers and Surfaces*, edited by E. Marinero (Materials Research Society, Pittsburg, 1995).
[16] W. Zhu, C. J. Hirschmugl, A. D. Laine, B. Sinkovic, and S. S. P. Parkin, Appl. Phys. Lett. **78**, 3103 (2001).
[17] V. G. Kravets, A. K. Petford-Long, and A. F. Kravets, J. Appl. Phys. **87**, 1762 (2000); V. G. Kravets, A. K. Petford-Long, and A. F. Kravetz, Physica E (Amsterdam) **4**, 292 (1999).
[18] M. Eßeling, Y. Luo, and K. Samwer, Europhys. Lett. **68**, 100 (2004).
[19] B. D. Cullity, *Elements of X-Ray Diffraction* (Addison-Wesley, London, 1978).
[20] H. Fujimori, in *Amorphous Metallic Alloys*, edited by F. E. Luborsky (Butterworths, London, 1983), p. 300.
[21] Davide Ceresoli and David Vanderbilt, Phys. Rev. B **74**, 125108 (2006).
[22] R. T. Mennicke, D. Bozec, V. G. Kravets, M. Vopsaroiu, J. A. D. Matthew, and S. M. Thompson, J. Magn. Magn. Mater. **303**, 92 (2006).
[23] C. F. Bohren and D. R. Huffman, *Absorption and Scattering of Light by Small Particles* (Wiley, New York, 1983).
[24] J. C. Maxwell Garnett, Philos. Trans. R. Soc. London, Ser. A **203**, 385 (1904).
[25] A. V. Sokolov, *Optical Properties of Metals* (Blackie, Glasgow, 1967).
[26] M. Schubert, T. E. Tiwald, and C. M. Herzinger, Phys. Rev. B **61**, 8187 (2000).
[27] T. Hirata, Phys. Rev. B **50**, 2874 (1994).
[28] K. Matsunaga, T. Tanaka, T. Yamamoto, and Y. Ikuhara, Phys. Rev. B **68**, 085110 (2003).
[29] R. E. Alonso, L. A. Errico, E. L. Peltzer y Blanca, A. Lopez-Garcia, A. Svane, and N. E. Christensen, Phys. Rev. B **78**, 165206 (2008).
[30] J. M. D. Coey, M. Venkatesan, P. Stamenov, C. B. Fitzgerald, and L. S. Dorneles, Phys. Rev. B **72**, 024450 (2005).
[31] W. H. Butler, X. G. Zhang, T. C. Schulthess, and J. M. MacLaren, Phys. Rev. B **63**, 054416 (2001).
[32] I. I. Oleinik, E. Yu. Tsymbal, and D. G. Pettifor, Phys. Rev. B **62**, 3952 (2000).